

First Row Transition Metal Oxide Based Catalysts for the In-situ Reactions

of Methanation and Desulfurization in the Removal of Sour Gases

from Simulated Natural Gas

Wan Azelee Wan Abu Bakar, Mohd. Yusuf bin Othman, Ching Kuan Yong & Junaidi Mohd. Nasir

Department of Chemistry, Faculty of Science

Universiti Teknologi Malaysia

81310 UTM Skudai, Johor, Malaysia

Tel: 60-13-746-6213 E-mail: wanazelee@yahoo.com

The research is financed by Universiti Teknologi Malaysia and Ministry of Science, Technology and Innovation, Malaysia through IRPA Vot 74248.

Abstract

The objective of this novel catalyst development is to achieve both low temperature and high conversion of sour gases of H_2S and CO_2 present in the natural gas. The results showed that the conversion of H_2S to elemental sulfur on all of the potential catalysts was achieved 100 %. However, methanation of CO_2 in the presence of H_2S yielded 0.7 % CH_4 over Fe/Zn/Cu/Ti-Al₂O₃ catalyst, 1.1 % CH_4 over Fe/Zn/Cu-Al₂O₃ catalyst and the highest is 6.1 % CH_4 over Pr/Co/Ni-Al₂O₃ catalyst at maximum studied temperature of 300 °C. The catalysts were further characterized by X-rays Photoelectron Spectroscopy and Nitrogen Adsorption analysis. XPS results revealed Ni²⁺ ion in the NiO and Ni³⁺ in Ni₂O₃ species, spinel compound of Co_3O_4 on the Pr/Co/Ni-Al₂O₃ catalyst. N₂ adsorption-desorption analysis illustrated 7.9 % increment of surface area over the spent Pr/Co/Ni-Al₂O₃ catalyst, which assumed to be responsible for the dramatical increased of the methanation activity of this catalyst at the reaction temperature of 300 °C.

Keywords: Titanium, Copper, Nickel, Methanation, Desulfurization, Natural gas

1. Introduction

Crude natural gas is categorized as a sour gas due to the contamination of carbon dioxide (CO_2) and hydrogen sulfide (H_2S). These corrosive elements may deteriorate the pipeline systems and become a safety hazard and also contribute to the environmental issue. Recently, the removal of these sour gases via chemical conversion techniques becomes the most promising technique. The catalysts for the CO_2 methanation have been extensively studied because of their application in the conversion of CO_2 gas to produce methane, which is the major component in natural gas. However, the presence of H_2S in the natural gas and certain industrial processes is known to cause poisoning of the metal surface with both sulfur and hydrogen.

The essential requirement for the correct selection of the oxide system is its ability to accept and to activate CO_2 and H_2S . The acid nature of CO_2 and H_2S necessitates the employment of a catalytic system with basic properties. Such requirements are met with some transition metal oxides and apparently some Lanthanide oxides. Their acid and redox properties may be changed by adding other oxides (Krylov *et al.*, 1998). Investigation done by Wang *et al.* (2007) found that the adsorption strength of CO_2 is controlled by the Lewis basicity of a catalyst, *d*-band center of the metal surface, charge transfer from the metal surfaces to the chemisorbed CO_2 . The major reason for the much slower of the catalyst science of mixed metal oxide is its significantly complexity compared with metal based catalyst, e.g. possible presence of multiple oxidation states, variable local coordination, coexisting bulk and surface phases as well as different surface termination functionalities such as M-OH, M=O or M-O-M (Wachs, 2005). Metal oxides are less active than metals, but they are stable in catalytic conditions.

Praseodymium oxide has been investigated as the most effective rare earth metal oxide when it was dopped onto NiO based catalyst for CO_2 methanation reaction at 400 °C. Later, cobalt oxide was found as the most suitable dopant towards the Pr/Ni catalyst (Wan Abu Bakar, 2005). Kulshreshtha *et al.* (1990) have been reported that Fe-Ti-Sn intermetallics are capable of CO methanation and almost completely converted CO to methane at 323 °C. This investigation concluded that the catalytic activity of the intermetallics is significantly improved by Sn substitution. Later, Pineda *et al.* (1997) found

out when zinc oxide and zinc ferrite catalysts were dopped with Cu and Ti, their catalytic performance on H_2S desulfurization process could be increased. The addition of Ti may increase the stability of ZnO towards reducing agent such as H_2 . However, the addition of Cu do not affect the stability of catalyst but improve the catalyst performance by changing the surface of the catalyst during calcination and activation process. It has been found that CO₂ strongly chemisorbs on the Fe (110) surface with the strongest binding energy, whereas CO₂ has moderate strength on the (111) surface of Co, Ni, Rh, Pd with slightly positive binding energies (Wang *et al.*, 2007). The selection of support is considered as important since it may influence both the activity and selectivity of the reaction. It has been discovered that the addition of alumina may increase the methanation activity although there is a presence of low concentration of H_2S (Happel & Hnatow, 1981). Therefore, Al_2O_3 is selected as the support for all of the studied catalysts in this research.

Efforts to search for efficient catalyst and to explore new technology in order to meet the demands of the economical feasibility of in-situ reactions of methanation and desulfurization for the purification of natural gas have not been extensively studied. The objective of this novel catalyst development is to achieve both low temperature and high conversion of sour gases. At low temperature, application of the novel catalyst in gas industry is more likely. However, problem arises because exothermic reaction of conversion of CO_2 to CH_4 is unfavorable at low temperature due to its low energy content.

2. Experimental

2.1 Preparation of catalysts

The catalysts were prepared by impregnation method, namely, impregnating appropriate amount of metal nitrate salts on Al_2O_3 beads support for 15 minutes and dried at 80°C for 24 hours. It was then calcined in air at 400°C for 5 hours. Ti⁴⁺ sol for the Ti based catalyst was prepared by dissolving 6 g of polyethylene glycol (PEG) with 600 mL ethanol. Then, 31.8 g diethanolamine (DEA) followed by 85.2 g titanium (IV) isopropoxide (Ti(iso)₄) was added when PEG completely dissolved. After that, 5.4 mL of distilled water was added and stirred for 10 minutes to get a homogeneous solution. Al₂O₃ beads were dipped into the Ti⁴⁺ sol and then dried in the oven at 80°C for 30 minutes. The following metal oxides were impregnated onto the Al_2O_3 according to the above said method.

2.2 Catalytic activity measurements

In-situ reactions of methanation and desulfurization was performed from room temperature up to 300 °C with temperature rate of 5 °C/ min. CO_2 and H_2 gases were introduced into the reactor system in a stoichiometric ratio of 1: 4. About 2.5 mL/ min H_2S gas was introduced into the gas stream. This composition is similar to the content of sour gases in Malaysian natural gas, which is 5 % of H_2S and 20 % of CO_2 . Screening on the produced gas stream was done by using FTIR analysis. Percentage conversion of CO_2 and H_2S was obtained by calculating the peak area of their respective stretching band. Off line Gas Chromatography analysis was done on the product gas to determine the selectivity and yield of CH_4 gas due to the low sensitivity of FTIR towards stretching band of CH_4 .

2.3 Characterization of catalysts

2.3.1 X-rays Photoelectron Spectroscopy

The potential catalysts were characterized by using Kratos instrument XSAM HS surface analysis spectrometer with Mg K α X-rays source (1253.6 eV). Sample was introduced into the spectrometer in flowing argon atmosphere, and evaporated at least 6 × 10⁹ Torr before spectrum was recorded. The spectrum was taken at 10 mA and 14 kV energy source at 2 sweeps.

2.3.2 Nitrogen Adsorption Analysis

The N₂ adsorption-desorption isotherms for the catalysts were measured by Micromeritics ASAP 2010. All samples were evacuated at 120 °C prior to the measurement. The specific surface area was calculated using the BET method. The total pore volume was determined at a relative pressure of P/ $P_0 = 0.99$.

3. Results and Discussion

3.1 In-situ reactions of CO₂ methanation and H₂S desulfurization

Figure 1 shows the details trend on the percentage conversion of CO_2 and H_2S over the potential Pr/Co/Ni (5: 35: 60)- Al_2O_3 , Fe/Zn/Cu (4: 16: 80)- Al_2O_3 and Fe/Zn/Cu/Ti (5: 5: 40: 50)- Al_2O_3 . Table 1 shows the yield of CH_4 which indicated the methanation activity of the studied catalysts.

Fe/Zn/Cu/Ti (5: 5: 40: 50)-Al₂O₃ catalyst showed a relatively higher H₂S conversion activity than the other two catalysts at temperature lower than 200 °C. It could be assigned as the best H₂S desulfurization catalyst among the studied catalysts due to its ability to convert higher percentage of H₂S at light off temperature. Pineda *et al.* (1997) have reported the presence of Ti may increase the H₂S desulfurization process at lower temperature. It had been proven that TiO₂ could influence the dissociation of H₂S to H⁺ and HS⁻ at the early stage due to its weak electron interaction in the *d* orbital (Blesa *et al.*, 1993). The graph in Figure 1 shows a decrease on the conversion of H₂S over Fe/Zn/Cu-Al₂O₃ and Fe/Zn/Cu/

Ti-Al₂O₃ catalysts from room temperature to 40 °C. This phenomenon was assigned to the adsorption of H₂S by the catalysts at lower temperature. Both the catalysts, completely removed H₂S at reaction temperature of 100 °C. At temperature higher than 200 °C, the H₂S desulfurization activity decreased in a great order over Fe/Zn/Cu-Al₂O₃ and Fe/Zn/Cu/Ti-Al₂O₃ catalysts. This may due to the uptake of H₂ by sulfur deposited on the surface of the catalysts to form H₂S. Therefore, H₂S desulfurization reaction at temperature higher than 200 °C is unfavored over these two catalysts. On the other hand, Pr/Co/Ni-Al₂O₃ catalyst showed a totally different trend in the conversion of H₂S compared to the copper and titanium oxide based catalysts. The conversion of H₂S over this catalyst gradually increased by the increasing of temperature until 100 % conversion of H₂S was achieved at reaction temperature of 280 °C.

During CO₂ methanation in the presence of H₂S, all the three catalysts showed a gradual increase until maximum studied temperature of 300 °C. Pr/ Co/ Ni-Al₂O₃ and Fe/ Zn/ Cu-Al₂O₃ catalysts yielded the same amount of CH₄ at reaction temperature of 200 °C (0.7 %), but Pr/ Co/ Ni-Al₂O₃ catalyst performed dramatically high CO₂ methanation and H₂S desulfurization activities at 300 °C. Pr/ Co/ Ni-Al₂O₃ gave the highest conversion of CO₂ where it converted 19.2 % of CO2 and yielded 6.1 % of CH4 at 300 °C. It is believed that Pr was able to generate active sites for the in-situ reactions of CO₂ and H₂S conversion at higher temperature. Rare earth metal oxides may increase the stability of catalyst at high temperature and avoid the sintering of nickel (Miao et al., 1997). At 300 °C, Fe/Zn/Cu-Al₂O₃ catalyst converted 12.7 % of CO₂ and yielded 1.1 % of CH₄. Fe/ Zn/ Cu/ Ti-Al₂O₃ catalyst yielded no CH₄ at 100 °C and gave only 0.7 % of CH₄ at 300 °C. The CO₂ methanation activity over this catalyst is considered very low. Basu et al. (2004) have proven that the addition of TiO at a high concentration may increase the surface oxygen storage. However, this property did not assist the adsorption of CO₂ on the catalyst surface. Besides that, the interaction between Ti and H₂ is weak because H₂ prefer to adsorb on the defect TiO lattice. Thus prevent the adsorption of H₂ during CO₂ methanation (Henrich & Cox, 1994). It has also been reported by Fournier (1986) that CH₄ formation from C is easier on Co (100) than Fe (110). The presence of subsurface C tends to increase the activation energy required for the hydrogenation steps and hence CH₄ formation becomes more difficult in the presence of Fe-carbides. Miao et al. (1997) also suggested that the interaction between transition metal and Al_2O_3 support is one of the most important factors that determined the redox ability. Nickel oxide based catalyst is the most suitable for the in-situ reactions of CO₂ methanation and H₂S desulfurization according to the results obtained in Figure 1 and Table 1.

3.2 Characterization of Catalysts

3.2.1 X-rays Photoelectron Spectroscopy (XPS)

The surface active components on the fresh and after catalytic testing (spent) catalysts of Pr/ Co/ Ni (5: 35: 60)-Al₂O₃, Fe/ Zn/ Cu (4: 6: 80)-Al₂O₃ and Fe/ Zn/ Cu/ Ti (5: 5: 40: 50)-Al₂O₃ were accomplished through XPS. All data was corrected by using the binding energy, $E_{\rm b}$, of C 1s at 284.5 eV as standard.

The E_b resulted from deconvolution peaks of Ni (2p) and Co (2p) from Pr/ Co/ Ni-Al₂O₃ was depicted in Table 2. The E_b of each species observed in Ni (2p) region for the fresh Pr/ Co/ Ni-Al₂O₃ catalyst are characteristic of the Ni²⁺ ion from the NiO at the E_b of 854.2 eV (2p_{3/2}) and 871.8 eV (2p_{1/2}), similar assignment to the data obtained made by Nefedov *et al.* (1975) who investigated on some coordination compounds; and Lorenz *et al.* (1979) who studied ESCA on NiO/ SiO₂ and NiO-Al₂O₃/ SiO₂ catalysts. The existence of Ni (2p) peak at 856.8 eV (2p_{3/2}) and 874.3 eV (2p_{1/2}) was attributed to the presence of Ni³⁺ in Ni₂O₃. Ni³⁺ shows a higher binding energy because the E_b of the metal increases when the covalency decreases (Vederine *et al.*, 1978). As the ionic radius of Ni²⁺ > Ni³⁺ and furthermore the covalency of Ni³⁺ decreases compare to Ni²⁺. It is known that Ni³⁺ is more reactive than Ni²⁺. It could be suggested that Ni₂O₃ at reaction temperature below 200 °C may be resulted from the lack of Ni₂O₃ present, which is an oxygen rich compound. XPS data also revealed the presence of spinel compound, Co₃O₄ on the surface of the catalyst, which is in accord with those reported by Kim (1975), Zeng *et al.* (1995), and Riedel & Schaub (2003) who worked with the CoO, CoO-ZrO₂ and Co Fischer-Tropsch catalyst, respectively. The existence of the spinel compound in the catalyst was assigned to be good for the catalytic efficiency as it provides more active sites for the reaction and also it can easily change forms according to the environment, whether it is more to Co²⁺ or Co³⁺.

After the exposure to the in-situ reactions of CO₂ methanation and H₂S desulfurization environment, NiO was disappeared in the spent catalyst. Similar phenomenon also reported by Djaidja *et al.* (2000). NiO phase was disappeared in their used Ni/ Sm₂O₃ and Ni/ La₂O₃ catalysts. Ni₂O₃ was detected in both of their fresh and used catalysts and they suggested that Ni₂O₃ phase is needed in the oxidative transformation of methane reaction course. The absence of NiO was presumably contributed to the increasing of the catalytic performance over this catalyst at maximum study temperature of 300 °C. The Co (2p) peaks shifted to a lower E_b of 778.7 eV (2p_{3/2}) and 782.8 eV (2p_{1/2}) indicating no changes in the Co oxidation state on the surface.

According to the XPS analysis, 0.7 % of Pr was available on the fresh Pr/ Co/ Ni-Al₂O₃ catalyst, while only 0.2 % of Pr was available on the spent catalyst. This reduction may due to the agglomeration of other elements that forced the Pr element to move into the bulk of the catalyst.

Even though the EDX analysis revealed the weight percentage of Zn as 0.2 % in the Fe/Zn/Cu-Al₂O₃ catalyst, no peak assigned to Zn was detected from the deconvolution peak of Zn. This may due to the agglomeration of the other elements, which thus pushed Zn into the lattice structure of the catalyst or poisoning from carbon compound during XPS analysis. The lower loading of Zn that is insensitive to the XPS analysis is also a factor. The E_b resulted from deconvolution peaks of Cu (2p) and Fe (2p) from Fe/Zn/Cu-Al₂O₃ catalyst was tabulated in Table 3. The fresh Fe/Zn/Cu-Al₂O₃ catalyst contained normal spinel compound of CuFe₂O₄. This spinel compound turned to inverse spinel structure after the catalytic testing. A normal spinel compound is the active site for this catalyst. Fe³⁺ made up the octahedral site while Cu²⁺ made up the tetrahedral site (Ando *et al.*, 1998a; 1998b) as illustrated in Figure 2. Peaks referred to normal spinel compounds of CuFe₂O₄ or Fe₃O₄ appeared at E_b of 710.1 eV (2p_{3/2}) and 723.7 eV (2p_{1/2}). CuFe₂O₄ and Fe₃O₄ were assumed to act as active species on the surface. Fe₃O₄ is considered as the more dominant structure compared to CuFe₂O₄. The spent Fe/Zn/Cu-Al₂O₃ catalyst showed deconvolution peaks of CuFe₂O₄ or Fe₃O₄ at E_b of 710.1 eV (2p_{3/2}) and 723.7 eV (2p_{1/2}). and 723.7 eV (2p₂O₄ and Fe₃O₄ and it is also the active site for H₂S desulfurization. Peak area of these peaks is high enough, which indicated the formation of surface Fe in a large amount. This also proved that Fe₃O₄ is a more dominant structure compared to CuFe₂O₄. The spent Fe/Zn/Cu-Al₂O₃ catalyst showed deconvolution peaks of CuFe₂O₄ or Fe₃O₄ at E_b of 710.1 eV (2p_{1/2}) but with 85.3 % reduction of peak area. This may due to the inverse spinel structure that contributed to the presence of larger amount of surface copper.

Normal spinel compound of CuFe₂O₄ was revealed from the deconvolution peak of Cu (2p) for the fresh and spent Fe/Zn/ Cu/Ti-Al₂O₃ catalysts (Table 4). Peaks referred to normal spinel compounds of CuFe₂O₄ or Fe₃O₄ appeared at E_b of 709.7 eV $(2p_{3/2})$ and 723.2 eV $(2p_{1/2})$ on the fresh Fe/Zn/Cu/Ti-Al₂O₃ catalyst. There are another peaks at E_b of 712.4 eV $(2p_{3/2})$ and 726.1 eV $(2p_{1/2})$ assigned to the Fe³⁺ bound to hydroxyl group (OH) in agreement with Shah *et al.* (2002). The higher binding energy of these peaks is due to the high electronegativity of hydroxyl group. OH ligand is more electronegative than oxygen. The presence of hydroxyl ligand could increase the oxidation reaction over Fe/Zn/Cu/Ti-Al₂O₃ catalyst due to its high electron density nature. Morrison (1998) also proved that TiO₂ in Fe/Zn/Cu/Ti-Al₂O₃ catalyst contributed to the presence of $Fe^{3^{+}}$ -OH and thus active site for the H₂S desulfurization. The adsorption process of H₂S at low temperature that may inhibit H₂S desulfurization could be avoided. On the other hand, the spent Fe/ Zn/ Cu/ Ti-Al₂O₃ catalyst also showed a lower peak area for deconvolution peaks of $CuFe_2O_4/Fe_3O_4$ at 710.5 eV ($2p_{3/2}$) and 724.1 eV $(2p_{1/2})$. This may resulted from carbon coking on the surface of the catalyst during XPS analysis or the formation of CuO obstructed the distribution of Fe on the catalyst surface. Similar with Fe/Zn/Cu-Al₂O₃ catalyst, no peak assigned to Zn was detected even though 0.1% of Zn was revealed by EDX analysis. In addition, the presence of Ti in the Fe/ Zn/ Cu/ Ti-Al₂O₃ catalyst also could not be detected due to the narrow diameter of Ti compared to Cu and Fe. It is believed that Ti was left inside the lattice structure of the catalyst. The interaction of electron from Ti is weak due to the distance of Ti inside the catalyst structure is comparably farer than those species on the surface.

3.2.2 Nitrogen Adsorption Analysis

One of the most characteristic properties of the surface of a solid is its ability to adsorb gases and vapours. Table 5 summarized the BET surface area and BJH desorption average pore diameter of the fresh supported catalysts and after in-situ reactions testing catalysts (spent catalysts). The fresh catalysts showed relatively narrower pore size compared to the spent catalysts. It is believed that some of the pores collapsed during the in-situ reactions of CO₂ methanation and H₂S desulfurization leading to the enlargement of the pores. From the BET surface area analysis, the surface area of the spent Pr/ Co/ Ni-Al₂O₃ catalyst is higher than the fresh catalyst. This could explain the dramatical increased of the methanation activity of this catalyst at the reaction temperature of 300 °C. It is assumed that the increasing of the surface area with respect to temperature finally increase the catalytic activity of the Pr/ Co/ Ni-Al₂O₃ catalyst at higher temperature. By referring to the XPS analysis, Co ions were detected as spinel compound of Co_3O_4 on the surface. It is believed that Co_3O_4 contributed to the increment of surface area over this catalyst. Besides that, NiO might play a role too. NiO is present in the fresh Pr/ Co/ Ni-Al₂O₃ catalyst but absent in the spent Pr/ Co/ Ni-Al₂O₃ catalyst. It was observed that Fe/Zn/Cu/Ti-Al₂O₃ catalyst posseses the highest surface area and narrowest pore size. This was supported by Yamasaki *et al.* (1999) that the addition of TiO_2 in the catalyst may increase the surface area and decrease the particle size. These features increased the H_2S desulfurization activity but not the CO_2 methanation activity. However, the catalytic activity of a particular catalyst not only depends on the BET surafce area and pore size, but also included other factors such as type of pores, shape of pores and the degree of porosity (Wan Abu Bakar, 2000). The Fe/ Zn/ Cu-Al₂O₃ catalyst showed reduction of 34 % and Fe/Zn/Cu/Ti-Al₂O₃ catalyst showed reduction of 17 % in surface area after undergoing catalytic testing. This reduction is possibly due to the sulfur poisoning on the surface of the catalysts during H₂S desulfurization, or collapsed of the pores during prolongs catalytic reaction. This was also proven by the Energy Dispersive X-rays Analysis, which indicated the appearance of sulfur element. However, the isotherm plot of the fresh and spent catalysts did not show significant difference. All the catalysts showed Type IV isotherm plot and H3 type hysteresis loop.

4. Conclusion

Nickel oxide based catalyst is the most potential for the in-situ reactions of CO_2 methanation and H_2S desulfurization compared to the copper oxide and titanium oxide based catalysts. It is capable of 100 % conversion of H_2S to elemental sulfur and yielded 6.1 % of CH_4 at reaction temperature of 300 °C. The aim to obtain high H_2S desulfurization rate at low temperature was achieved. However, improvement is needed for the CO_2 methanation reaction. Therefore, further efforts are needed in the future work in the attempt to obtain catalysts that may increase the conversion rate of CO_2 and H_2S simultaneously at much lower temperature.

References

Ando, H., Fujiwara, M., Matsumura, Y., Miyamura, H., Tanaka, H. & Souma, Y. (1998a). Methanation of Carbon Dioxide over LaNi₄ X-Type Intermetallic Compounds as Catalyst Presursor. *Journal of Alloys and Compounds*, 223, 139-141.

Ando, H., Qiang, X., Fujiwara, M., Matsumura, Y., Tanaka, H. & Souma, Y. (1998b). Hydrocarbon Synthesis from CO₂ over Fe-Cu Catalysts. *Catalysis Today*, 45, 229-234.

Basu. B., Vleugels, J. & Der Biest, O.V. (2004). Transformation Behaviour of Tetragonal Zirconia: Role of Dopant Content and Distribution. *Materials Science and Engineering A*, 366, 338-347.

Blesa, M.A., Morando, P.J. & Regazzoni, A.E. (1993). Chemical Dissolution of Metal Oxides. Florida, United States of America: CRC Press, Inc., 269-272.

Djaidja, A., Barama, A. & Bettahar, M.M. (2000). Oxidative transformation of methane over nickel catalysts supported on rare-earth metal oxides. *Catalysis Today*, 61, 303-307.

Fournier, J. A. (1986). Characterization of some iron catalysts for the reduction of carbon monoxide and the effect of residence time and temperature on the nature of carbon monoxide reduction products. PhD Thesis. Brown University, United States of America.

Happel, J. & Hnatow, M. A. (1981). U.S. Patent 4, 260, 553. Washington DC: U.S. Patent and Trademark Office.

Henrich, V.E. & Cox, P.A. (1994). The Surface Science of Metal Oxides. Cambridge University Press, Great Britain, 128-138.

Kim, K.S. (1975). X-ray Photoelectron Spectroscopics studies of the electronic structure of CoO. *Physical Review B*, 11 (6), 2177-2187.

Krylov, O.V., Mamedov, A.Kh. & Mirzabekova, S.R. (1998). Interaction of carbon dioxide with methane on oxide catalysts. *Catalysis Today*, 42, 211-215.

Kulshreshtha, S. K., Sasikala, R., Gupta, N. M. & Iyer, R. M. (1990). Carbon monoxide methanation over FeTi_{1-x}Sn_x intermetallics: Role of second phase. *Catalysis Letter*, 4 (2), 129-138.

Lorenz, P., Finster, J., Wendt, G., Salyn, J.V., Žumadilov, E.K. & Nefedov, V.I. (1979). ESCA investigations of some NiO/SiO₂ and NiO-Al₂O₃/SiO₂ catalysts. *Journal of Electron Spectroscopy and Related Phenomena*, 16, 267-276.

Miao, O., Xiong, G.X., Sheng, S.S., Cui, W., Xu, L., & Guo, X.X. (1997). Partial oxidation of methane to syngas over nickel-based catalysts modified by alkali metal oxide and rare earth metal oxide. *Applied Catalysis A: General*, 154, 17-27.

Morrison, S.R. (1998), Chemisorption on Nonmetallic Surface. In: Anderson, J.R. and Boudart, M. (eds). *Catalytic Science and Technology*, 3, 199-229.

Nefedov, V.I., Gati, D., Dzhurinskii, B.F., Sergushin, N.P. & Salyn, Ya.V. (1975). Simple and coordination compounds. *Russian Journal of Inorganic Chemistry*, 20, 2307-2314.

Pineda, M., Fierro, J. L. G., Palacios, J. M., Cilleruelo, E. G. & Ibarra, J. V. (1997). Characterization of Zinc Oxide and Zinc Ferrite Doped with Ti and Cu as Sorbents for Hot Gas Desulfurization. *Applied Surface Science*, 119, 1-10.

Riedel, T. & Schaub, G. (2003). Low-temperature Fisher-Tropsch synthesis on cobalt catalyst-effects of CO₂. *Topics in Catalysis*, 26 (1-4), 145-155.

Shah, P., Shoma, M., Kawaguchi, K. & Yamaguchi, I. (2002). Growth Conditions, Structural and Magnetic Properties of $M/Fe_3O_4/I$ (M = Al, Ag and I = Al₂O₃ and MgO) Multilayers. *Journal of Magnetism and Magnetic Materials*, 214, 1-5.

Vederine, J.C., Hollinger, G. & Minh, O.T. (1978). Investigations of Antigorite and Nickel Supported Catalysts by X-ray Photoelectron Spectroscopy. *The Journal of Physical Chemistry*, 82, 1515.

Wan Abu Bakar, W.A. (2000). Personnel Communications. Universiti Teknologi Malaysia, Malaysia.

Wan Abu Bakar, W.A. (2005). Personnel Communications. Universiti Teknologi Malaysia, Malaysia.

Wachs, I.E. (2005). Recent conceptual advances in the catalysis science of mixed metal oxide catalytic materials. *Catalysis Today*, 100, 79-94.

Wang, S.G., Liao, X.Y., Cao, D.B., Huo, C.F., Li, Y.W., Wang, J.G. & Jiao, H.J. (2007). Factors controlling the interaction of CO₂ with transition metal surfaces. *Journal of Physical Chemistry C*, 111, 16934-16940.

Yamasaki, M., Komori, M. Akiyama, E., Habazaki, H., Kawashima, A., Asami, K. & Hashimoto, K. (1999). CO₂ Methanation Catalysts prepared from Amorphous Ni-Zr-Sm and Ni-Zr Misch Metal Alloy Precursors. *Material Science and Engineering A*, 267, 220-226.

Zeng, H.C., Lim, J. & Tan, K.L. (1995). Memory effect of ZrO₂ matrix on surface Co₃O₄-CO position. *Journal of Material Research*, 10, 3096-3105.

Table 1. Yields from in-situ reactions of CO₂ methanation and H₂S desulfurization over Al₂O₃ supported Pr/ Co/ Ni (5: 35: 60), Fe/ Zn/ Cu (4: 16: 80) and Fe/ Zn/ Cu/ Ti (5: 5: 40: 50) catalysts

Catalyst	Temperature	Convert	ted CO ₂ (%)	Unreacted CO ₂	
	(°C) –	CH ₄	$CO + H_2O$	(%)	
Pr/ Co/ Ni (5: 35:	100	0.4	10.7	88.9	
60)-Al ₂ O ₃	200	0.7	14.1	85.2	
	300	6.1	13.1	80.8	
Fe/ Zn/ Cu (4: 16:	100	0.6	5.9	93.5	
80)-Al ₂ O ₃	200	0.7	11.3	88.0	
	300	1.1	11.6	87.3	
Fe/ Zn/ Cu/ Ti (5: 5: 40:	100	0.0	0.7	99.3	
50)-Al ₂ O ₃	200	0.4	6.2	93.4	
	300	0.7	7.3	92.0	

Table 2. XPS data of Ni (2p) and Co (2p) for fresh and spent Pr/ Co/ Ni (5: 35: 60)-Al₂O₃ catalysts

Catalyst	Weight (%)	Binding Energy (eV) ^a		$\Delta E_{\rm SO}^{\rm b}$ (eV)	Peak Area ^c	Peak Assignment
		$2p_{3/2}$	$2p_{1/2}$		$(2p_{3/2})$	
Pr/ Co/ Ni (5:35:60)-Al ₂ O ₃	5.1	854.2	871.7	17.5	167.9	Ni ²⁺ in NiO
(fresh)		856.8	874.3	17.5	115.6	Ni ³⁺ in Ni ₂ O ₃
	1.6	779.8	794.0	14.2	127.6	Co ₃ O ₄
Pr/ Co/ Ni (5:35:60)-Al ₂ O ₃	7.6	856.8	874.3	17.5	233.3	Ni ³⁺ in Ni ₂ O ₃
(spent)	1.6	781.7	796.1	14.4	92.9	Co ₃ O ₄

^a Binding energy, $E_{\rm b}$ corrected by specific operation charge effect (284.5 eV)

^b ΔE_{SO} (difference of 2 spin orbit) = $E_b(2p_{1/2}) - E_b(2p_{3/2})$

^c Peak Area = Peak Intensity × FWHM (Full Width Half Maximum)

Catalyst	Weight (%)	Binding Energy (eV) ^a		ΔE_{so}^{b} (eV)	Peak Area ^c	Peak Assignment
		$2p_{3/2}$	$2p_{1/2}$	-	$(2p_{3/2})$	
Fe/ Zn/ Cu	1.8	933.7	953.6	19.9	21.6	CuFe ₂ O ₄
(4:16:80)-Al ₂ O ₃ (fresh)						(normal spinel)
	3.6	710.1	723.7	13.6	66.7	CuFe ₂ O ₄ / Fe ₃ O ₄
						(normal spinel)
Fe/ Zn/ Cu	4.2	935.1	954.9	19.8	23.9	CuFe ₂ O ₄
(4:16:80)-Al ₂ O ₃ (spent)						(inverse spinel)
	3.4	710.1	723.7	13.6	9.8	CuFe ₂ O ₄ / Fe ₃ O ₄
						(normal spinel)

Table 3. XPS data of Cu (2p) and Fe (2p) for fresh and spent Fe/ Zn/ Cu (4: 16: 80)-Al₂O₃ catalysts

^a Binding energy, E_b corrected by specific operation charge effect (284.5 eV)

^b ΔE_{SO} (difference of 2 spin orbit) = $E_b(2p_{1/2}) - E_b(2p_{3/2})$

^c Peak Area = Peak Intensity × FWHM (Full Width Half Maximum)

Table 4. XPS data of Cu (2p) and Fe (2p) for fresh and spent Fe/Zn/Cu/Ti (5: 5: 40: 50)-Al₂O₃ catalysts

Catalyst	Weight (%)	Binding (e ^v		$\frac{\Delta E_{\rm SO}^{\rm b}}{\rm (eV)}$	Peak Area ^c (2p _{3/2})	Peak Assignment
		2p _{3/2}	$2p_{1/2}$			
Fe/ Zn/ Cu/ Ti	3.6	933.6	953.5	19.9	247.6	CuFe ₂ O ₄
(5:5:40:50)-Al ₂ O ₃						(normal spinel)
(fresh)	3.8	709.7	723.2	13.5	12.5	CuFe ₂ O ₄ / Fe ₃ O ₄
						(normal spinel)
		712.4	726.1	13.7	6.4	Fe ³⁺ -OH
Fe/ Zn/ Cu/ Ti	3.7	933.7	953.5	19.9	59.9	CuFe ₂ O ₄
(5:5:40:50)-Al ₂ O ₃						(normal spinel)
(spent)	2.8	710.5	724.1	13.6	10.0	CuFe ₂ O ₄ / Fe ₃ O ₄ (normal spinel)

^a Binding energy, $E_{\rm b}$ corrected by specific operation charge effect (284.5 eV)

^b ΔE_{SO} (difference of 2 spin orbit) = $E_b(2p_{1/2}) - E_b(2p_{3/2})$

^c Peak Area = Peak Intensity × FWHM (Full Width Half Maximum)

Al ₂ O ₃ Supported Catalyst	Condition	$S_{\rm BET}^{a} ({\rm m}^2 {\rm g}^{-1})$	d ^b (nm)
Pr/ Co/ Ni = 5: 35: 60	Fresh	166.2	5.6
Pr/ Co/ Ni = 5: 35: 60	Spent	180.4	5.9
Fe/ Zn/ Cu = 4: 16: 80	Fresh	184.8	5.1
Fe/ Zn/ Cu = 4: 16: 80	Spent	121.6	7.1
Fe/ Zn/ Cu/ Ti = 5: 5: 40: 50	Fresh	259.2	2.6
Fe/ Zn/ Cu/ Ti = 5: 5: 40: 50	Spent	215.6	3.2

Table 5. BET surface area and BJH desorption average pore diameter of the fresh and after in-situ reactions testing catalysts

^a BET surface area

^b BJH desorption average pore diameter

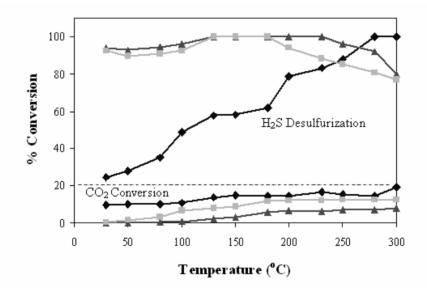


Figure 1. Percentage conversion of CO₂ and H₂S versus reaction temperature under in-situ reactions of CO₂ methanation and H₂S desulfurization over (\blacklozenge) Pr/ Co/ Ni (5: 35: 60)-Al₂O₃; (\blacksquare) Fe/ Zn/ Cu (4: 16: 80)-Al₂O₃; (\blacktriangle) Fe/ Zn/ Cu/ Ti (5: 5: 40: 50)-Al₂O₃ catalysts.

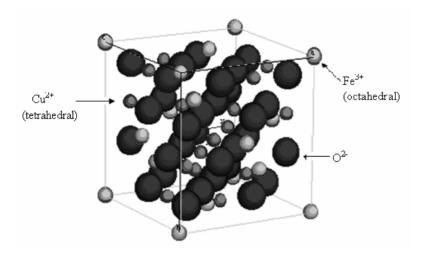


Figure 2. An illustration diagram of normal spinel compound of CuFe₂O_{4.}